

This document is confidential and is proprietary to the American Chemical Society and its authors. Do not copy or disclose without written permission. If you have received this item in error, notify the sender and delete all copies.

## Vapor-Deposited Ethylbenzene Glasses Approach “Ideal Glass” Density

Journal:	<i>The Journal of Physical Chemistry Letters</i>
Manuscript ID	jz-2019-01508x.R1
Manuscript Type:	Letter
Date Submitted by the Author:	26-Jun-2019
Complete List of Authors:	Beasley, Madeleine; University of Wisconsin Madison, Chemistry Bishop, Camille; University of Wisconsin Madison, Chemistry Kasting, Benjamin; University of Wisconsin Madison, Chemistry Ediger, Mark; University of Wisconsin Madison, Chemistry

SCHOLARONE™  
Manuscripts

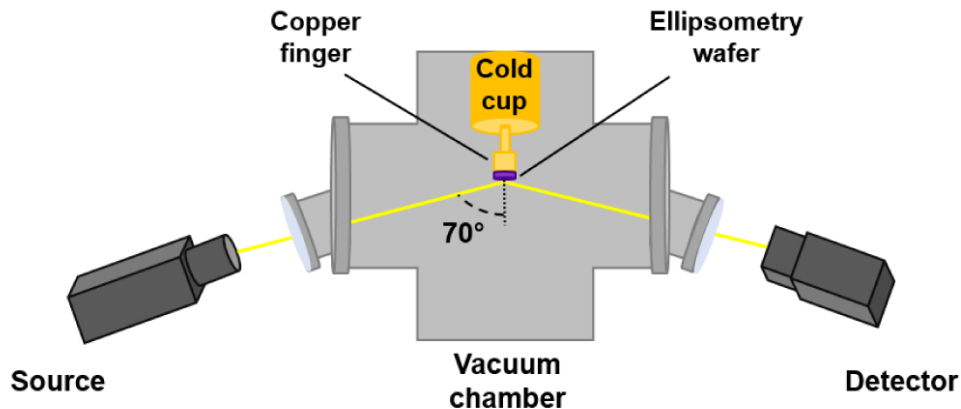


Figure 1. Schematic of in situ ellipsometry experiment. The source and detector are both fixed at a  $70^\circ$  angle relative to the surface normal of the silicon substrate.

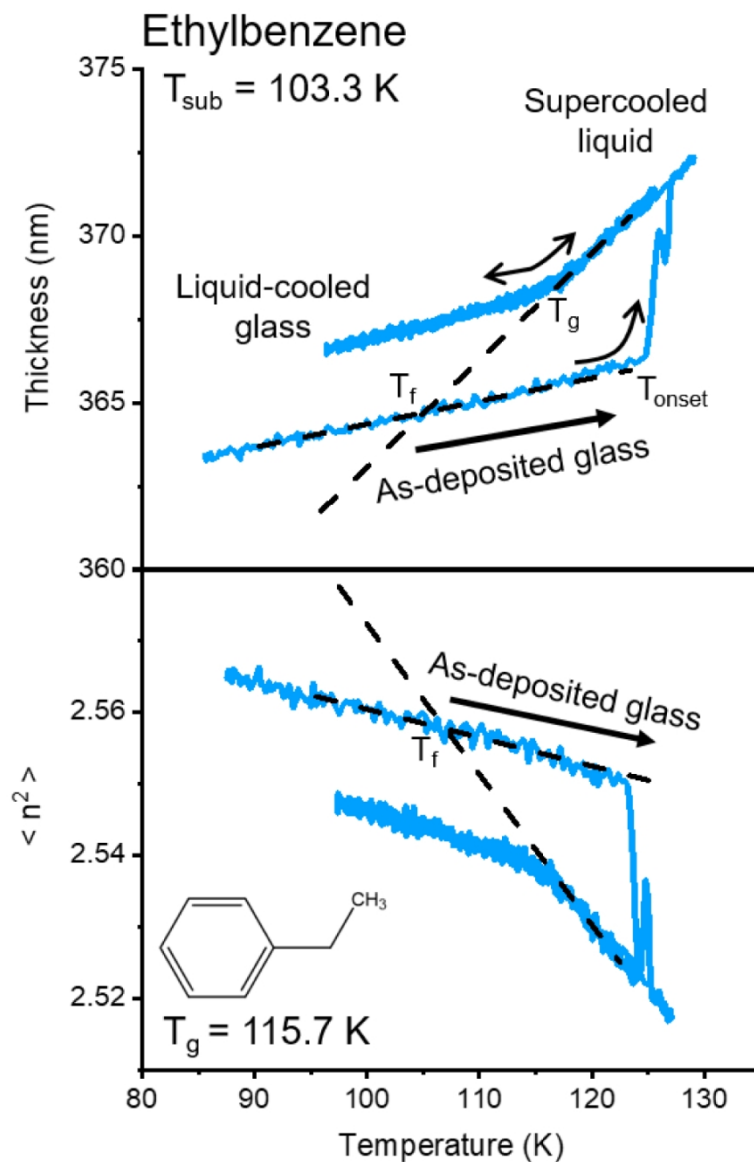


Figure 2. In situ ellipsometry data from ramping experiments of ethylbenzene deposited at  $T_{\text{sub}} = 103.3 \text{ K}$  ( $0.89 T_g$ ) with a rate of  $0.7 \text{ nm/s}$  illustrating the increased density and kinetic stability of the PVD glass. The top panel shows the thickness of the as-deposited glass in comparison with the liquid-cooled glass. The bottom panel shows mean-squared refractive index ( $\langle n^2 \rangle$ ). The black dashed lines are fits to the data for the glasses and supercooled liquid. The intersection of the extrapolated supercooled liquid line and as-deposited glass fit defines the fictive temperature,  $T_f$ . The intersection of the supercooled liquid and liquid-cooled glass fits define  $T_g$ . The structure of ethylbenzene is shown in the bottom panel.

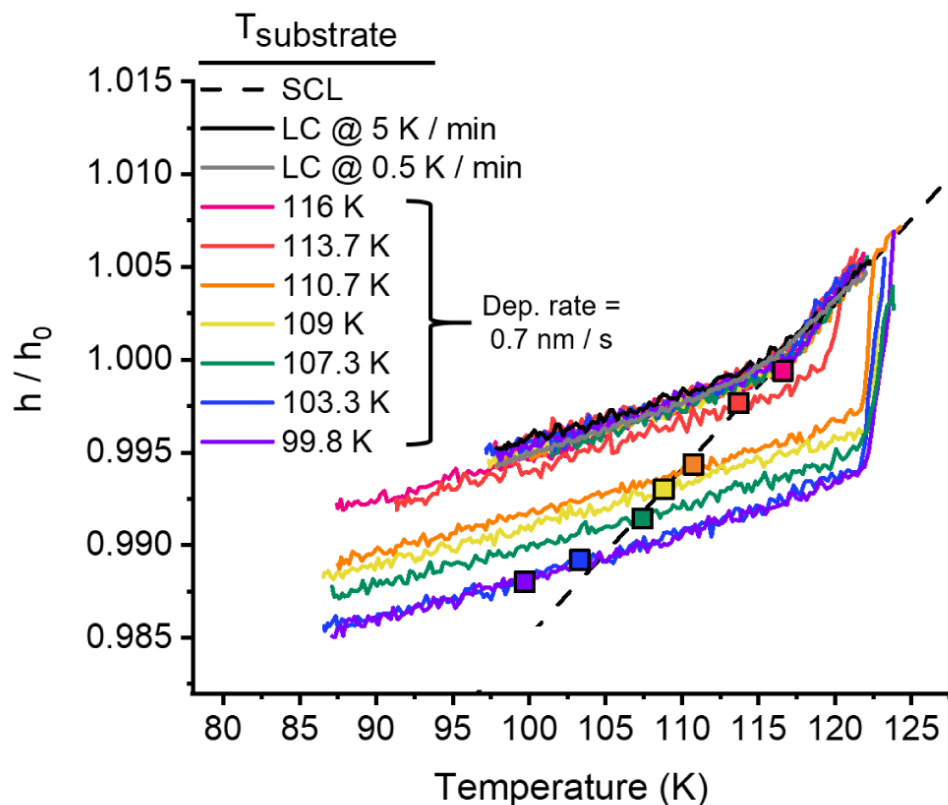


Figure 3. Normalized change in thickness as a function of temperature for glasses of ethylbenzene deposited at 0.7 nm/s. The colored curves represent PVD glasses prepared at the indicated substrate temperatures. The heating curve for the as-deposited glass and the first heating curve for the corresponding liquid-cooled glass are shown. The black and grey curves show results for liquid-cooled glasses cooled at 5 K/min and 0.5 K/min, respectively. The black dashed line is the extrapolation of the equilibrium supercooled liquid. Colored squares represent the normalized change in thickness at the deposition temperature. When these squares lie on the dashed line, the densities measured are consistent with the density expected for the supercooled liquid. For clarity, only the glasses prepared with a deposition rate of 0.7 nm/s are shown.

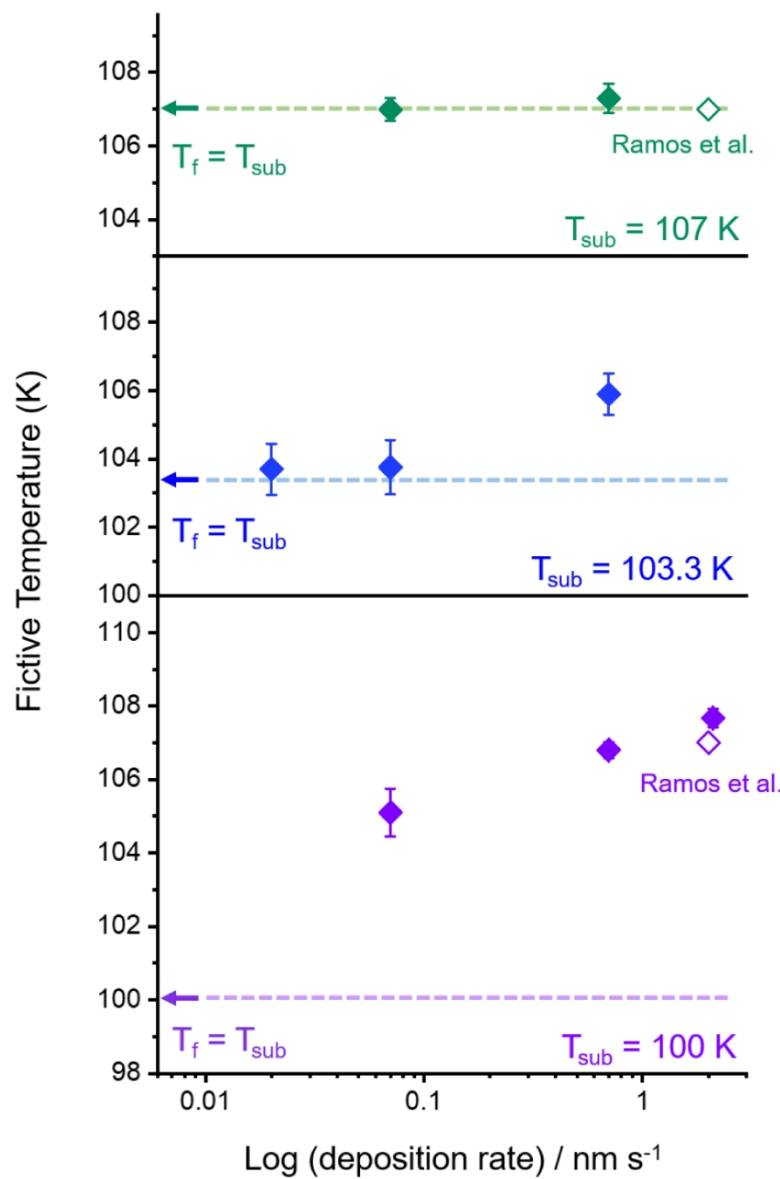


Figure 4. Fictive temperatures as a function of deposition rate for glasses deposited at 107 K (green, top), 103.3 K (blue, middle) and 100 K (purple, bottom). The solid points are fictive temperatures calculated from density measurements. Arrows and dashed lines indicate where  $T_f = T_{\text{sub}}$ . The open points represent enthalpy measurements by Ramos et al.<sup>32</sup>

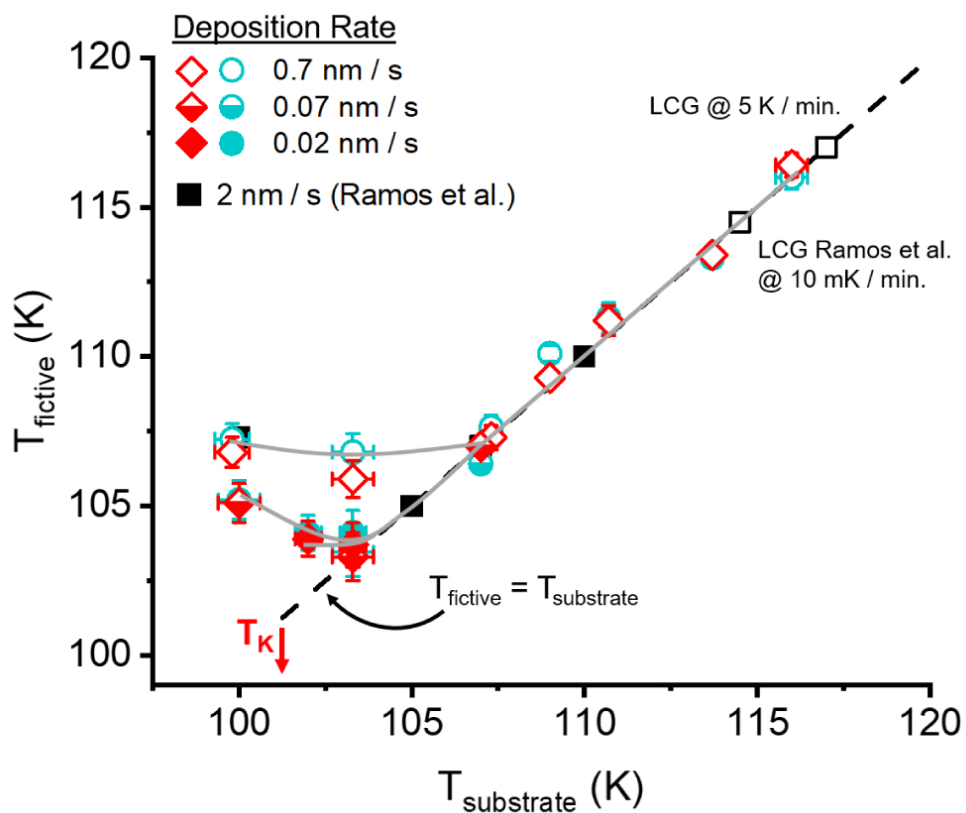


Figure 5. Fictive temperature as a function of substrate temperature during deposition for ethylbenzene glasses prepared at several rates. At low deposition rates, PVD glasses have the properties expected for the supercooled liquid to within 2 K of  $T_K$ . Red symbols are calculated from thickness measurements, teal symbols are calculated from refractive index measurements, and black squares from enthalpy measurements.<sup>32</sup> Open squares represent liquid-cooled glasses with cooling rates indicated. The arrow indicates the location of  $T_K$  as reported by Ref. 7. The grey solid lines are guides to the eye illustrating trends for different deposition rates.

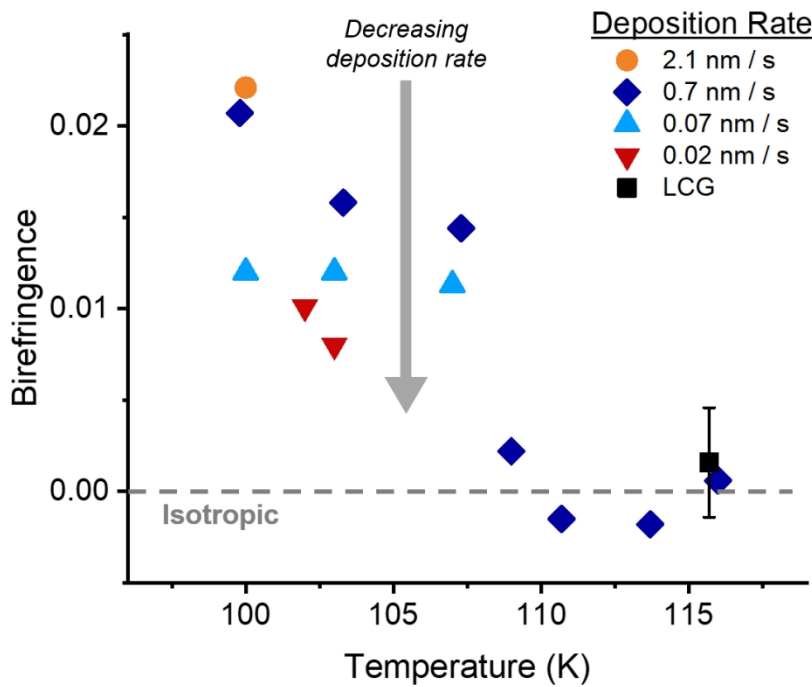


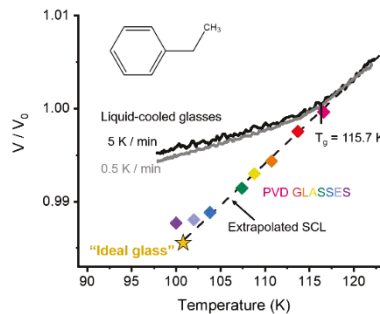
Figure 6. Birefringence as a function of substrate temperature for vapor-deposited glasses of ethylbenzene, with deposition rates indicated in the legend. The black open square is the average birefringence of all glasses prepared by cooling the liquid at 5 K/min; the error bar indicates one standard deviation. Error bars for the PVD glasses are expected to be comparable.

229x175mm (150 x 150 DPI)

1  
2  
3 Vapor-Deposited Ethylbenzene Glasses Approach “Ideal Glass” Density  
4 M.S. Beasley<sup>\*1</sup>, C. Bishop<sup>1</sup>, B.J. Kasting<sup>1</sup>, and M.D. Ediger<sup>1</sup>  
5  
6

7 <sup>1</sup>Department of Chemistry, University of Wisconsin-Madison, Madison, Wisconsin, 53706,  
8 United States  
9 \*Corresponding author  
10 To be submitted to the *Journal of Physical Chemistry Letters*

11  
12 **TOC Figure:**



**Abstract:** Spectroscopic ellipsometry was used to characterize vapor-deposited glasses of ethylbenzene ( $T_g = 115.7$  K). For this system, previous calorimetric experiments have established that a transition to the ideal glass state is expected to occur near 101 K (the Kauzmann temperature,  $T_K$ ) if the low temperature supercooled liquid has the properties expected based upon extrapolation from above  $T_g$ . Ethylbenzene glasses were vapor-deposited at substrate temperatures between 100 K ( $\sim 0.86 T_g$ ) and 116 K ( $\sim T_g$ ), using deposition rates of 0.02 – 2.1 nm/s. Down to 103 K, glasses prepared in the limit of low deposition rate have densities consistent with the extrapolated supercooled liquid. The highest density glass is within 0.15% of the density expected for the ideal glass. These results support the hypothesis that the extrapolated properties of supercooled ethylbenzene are correct to within just a few Kelvin of  $T_K$ , consistent with the existence of a phase transition to an ideal glass state at  $T_K$ .

1  
2  
3 Glasses are non-equilibrium materials and thus their properties depend upon how they are  
4 prepared. For example, for a typical liquid with a positive thermal expansion coefficient, the glass  
5 prepared by cooling at 1 K/min will be denser than the glass prepared by cooling at 10 K/min.  
6  
7 Slower cooling allows the liquid to remain in equilibrium down to lower temperatures where the  
8 density is higher. This scenario might suggest that the liquid density would continue to rise if the  
9 liquid could be equilibrated even as temperature approached  $T = 0$  K, but there are good reasons  
10 to think that this is not the case. Kauzmann described how the entropy provides a bound on the  
11 properties of the amorphous state.<sup>1</sup> The entropy of a supercooled liquid typically decreases more  
12 rapidly with temperature than does the crystal entropy. If this trend continued unabated down to  
13  $T=0$  K, the entropy of the liquid would be less than the entropy of the crystal, in violation of the  
14 3<sup>rd</sup> law of thermodynamics.<sup>2</sup> For understanding glass formation, it is useful to consider the  
15 configurational part of the liquid entropy as this quantity decreases rapidly with decreasing  
16 temperature and must remain positive. In the limit in which a liquid is cooled infinitely slowly, a  
17 number of scenarios have been suggested to avoid the configurational entropy crisis, including a  
18 phase transition to an “ideal glass” state at a temperature denoted the Kauzmann temperature  
19 ( $T_K$ ).<sup>3-4</sup> Conventionally,  $T_K$  is defined as the temperature where the extrapolated configurational  
20 entropy is zero. In this scenario, the ideal glass is the amorphous state with the lowest position on  
21 the potential energy landscape.

22  
23  
24  
25  
26  
27  
28  
29  
30  
31  
32  
33  
34  
35  
36  
37  
38  
39  
40  
41  
42  
43  
44  
45 One current theoretical approach supports the idea of a phase transition at  $T_K$ , positing a  
46 random first order transition to the ideal glass.<sup>5</sup> Some recent computer simulations support this  
47 scenario, showing a precipitous decrease of the liquid entropy as temperature is decreased and  
48 direct indications of an increasing structural length scale associated with this loss of entropy.<sup>6-7</sup>  
49  
50 While many experiments<sup>8</sup> are consistent with a transition to an ideal glass at  $T_K$ , this is clearly not  
51  
52  
53  
54  
55  
56  
57  
58  
59  
60

1  
2  
3 the only possible resolution to the entropy crisis.<sup>2</sup> Alternatively, a first-order phase transition could  
4 occur between  $T_g$  and  $T_K$ ; evidence for liquid-liquid transitions has been reported triphenyl  
5 phosphite<sup>9-10</sup>,  $Al_2O_3$ - $Y_2O_3$ <sup>11</sup>, and water.<sup>12-15</sup> The free volume models of Cohen and Grest<sup>16</sup> and the  
6  
7 cooperative bond-lattice excitation models of Angell<sup>17-18</sup> also suggest a first-order phase transition  
8 as the resolution to the entropy crisis. Another possibility, a continuous change in liquid properties,  
9 without a phase transition, has also been suggested;<sup>19</sup> behavior of this type has been obtained from  
10 two-state models<sup>20</sup> and computer simulations of specific systems.<sup>21-24</sup>  
11  
12

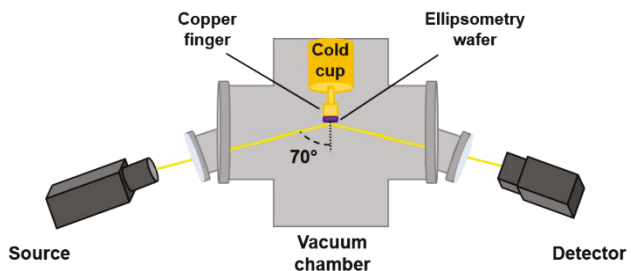
13 While it is important to understand the resolution to the Kauzmann entropy crisis, it is  
14 difficult to do so because the liquid must remain in equilibrium as  $T_K$  is approached. Liquids cooled  
15 from above the melting temperature get “stuck” on the energy landscape well above  $T_K$ ; as the  
16 system is cooled at a fixed rate, it falls out of equilibrium when the time required for molecular  
17 motion exceeds that available.<sup>25-26</sup> Since molecular motions slow down dramatically as  
18 temperature is lowered, cooling times well beyond experimental timescales would be required to  
19 attain equilibrium even halfway from  $T_g$  to  $T_K$ . This limitation naturally leaves the question “do  
20 supercooled liquids below the glass transition temperature have the properties expected by  
21 extrapolation?” unanswered. In order to understand how the entropy crisis might be resolved, non-  
22 traditional preparation techniques must be utilized to access states lower in the potential energy  
23 landscape. Experiments on geologically aged glasses<sup>27</sup> and swap Monte Carlo computer  
24 simulations are possible routes for approaching the ideal glass state.<sup>6-7</sup> The swap Monte Carlo  
25 simulations have been used to prepare equilibrium supercooled liquids down to much lower  
26 temperatures than previously possible,<sup>6-7</sup> and are consistent with a phase transition to an ideal glass  
27 state at  $T_K$ .<sup>28-30</sup>  
28  
29  
30  
31  
32  
33  
34  
35  
36  
37  
38  
39  
40  
41  
42  
43  
44  
45  
46  
47  
48  
49  
50  
51  
52  
53  
54  
55  
56  
57  
58  
59  
60

Physical vapor deposition (PVD) is a promising route for the preparation of glasses low on the potential energy landscape.<sup>31-34</sup> PVD glasses have properties expected for glasses cooled at extremely low rates since rapid surface equilibration during deposition allows the kinetic restrictions of bulk cooling to be circumvented. In 2011, Ramos et al. published high precision adiabatic calorimetry measurements on PVD glasses of ethylbenzene ( $T_g \approx 116$  K).<sup>33</sup> They found that glasses deposited at substrate temperatures from 105 to 110 K had the enthalpies expected for the extrapolated supercooled liquid at the given substrate temperatures and are thus very low in the potential energy landscape. One interpretation of these results is that, at the deposition rate used (2 nm/s), glasses vapor-deposited with substrate temperatures down to 105 K ( $T_K + 4$  K) are accurate models for the equilibrium supercooled liquid. Still, this calorimetry work left significant questions unanswered: Are the properties of these PVD glasses independent of deposition rate, as would be expected if equilibrium had been attained? Are PVD glasses of ethylbenzene structurally isotropic, as expected for the equilibrium supercooled liquid? Can glasses with properties consistent with the extrapolated supercooled liquid be obtained even closer to  $T_K$ ?

In order to answer these questions, we investigate how the densities of PVD glasses of ethylbenzene depend on a wide range of substrate temperatures and deposition rates. In addition to the work of Ramos et al.<sup>33</sup>, ethylbenzene has been well-characterized by dielectric spectroscopy<sup>35</sup>, adiabatic calorimetry<sup>25</sup>, nanocalorimetry<sup>34, 36-38</sup> light scattering experiments<sup>39-40</sup>, and atomistic simulations.<sup>41</sup> We find that glasses of ethylbenzene deposited at temperatures between 107 K and 116 K have densities consistent with the extrapolated supercooled liquid when prepared with deposition rates near 0.7 nm/s. In this temperature range, the enthalpy of PVD glasses of ethylbenzene is also consistent with high temperature extrapolations.<sup>33</sup> If slower deposition rates are used, either 0.07 nm/s or 0.02 nm/s, we can prepare ethylbenzene glasses at a

1  
2  
3 substrate temperature of 103 K that also have the density expected for the extrapolated supercooled  
4 liquid. Based on these results, we expect that PVD glasses can serve as accurate models for the  
5 equilibrium supercooled liquid. Our results support the hypothesis that the extrapolated properties  
6 of supercooled ethylbenzene are correct to within just a few Kelvin of  $T_K$ , consistent with the  
7 existence of a phase transition to an ideal glass state at  $T_K$ .  
8  
9  
10  
11  
12  
13

14  
15 *In situ* spectroscopic ellipsometry was used to characterize PVD glasses of ethylbenzene  
16 as schematically illustrated in Figure 1. Glass films roughly 400 nm thick were deposited onto a  
17 temperature-controlled silicon wafer. The ellipsometer source and detector were attached to the  
18 vacuum chamber and both fixed at a 70° angle relative to the surface normal of the silicon wafer.  
19  
20 The ellipsometric data were fit in the 350 – 1000 nm wavelength range to an anisotropic Cauchy  
21 model. Further modelling details are provided in the Methods section.  
22  
23  
24  
25  
26  
27  
28  
29  
30  
31  
32  
33  
34  
35  
36  
37  
38  
39  
40  
41  
42  
43  
44  
45



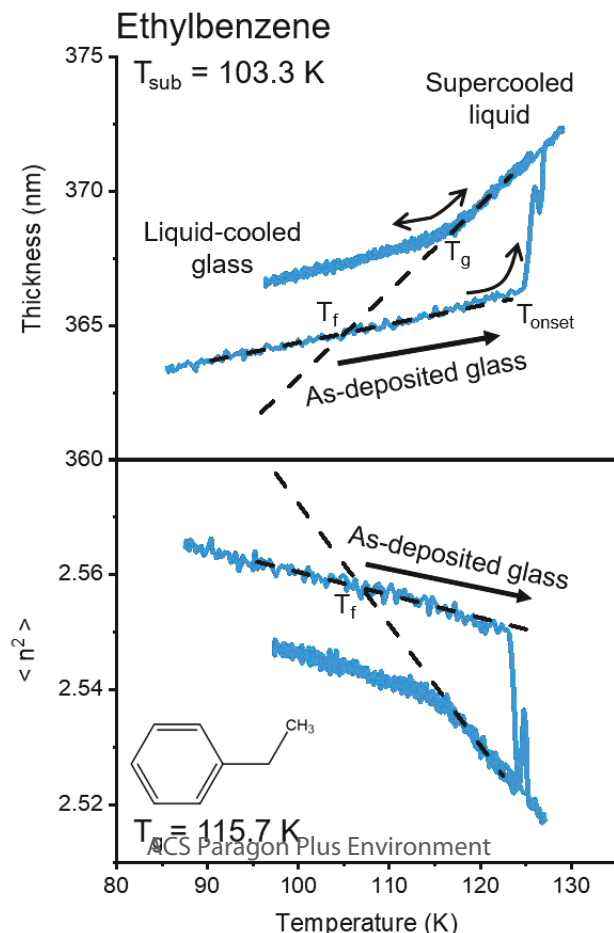
46  
47  
48  
49  
50  
51  
52  
53  
54  
55  
56  
57  
58  
59  
60 *Figure 1. Schematic of in situ ellipsometry experiment. The source and detector are both fixed at a 70° angle relative to the surface normal of the silicon substrate.*

61  
62  
63  
64  
65  
66  
67  
68  
69  
70  
71  
72  
73  
74  
75  
76  
77  
78  
79  
80  
81  
82  
83  
84  
85  
86  
87  
88  
89  
90  
91  
92  
93  
94  
95  
96  
97  
98  
99  
100  
101  
102  
103  
104  
105  
106  
107  
108  
109  
110  
111  
112  
113  
114  
115  
116  
117  
118  
119  
120  
121  
122  
123  
124  
125  
126  
127  
128  
129  
130  
131  
132  
133  
134  
135  
136  
137  
138  
139  
140  
141  
142  
143  
144  
145  
146  
147  
148  
149  
150  
151  
152  
153  
154  
155  
156  
157  
158  
159  
160  
161  
162  
163  
164  
165  
166  
167  
168  
169  
170  
171  
172  
173  
174  
175  
176  
177  
178  
179  
180  
181  
182  
183  
184  
185  
186  
187  
188  
189  
190  
191  
192  
193  
194  
195  
196  
197  
198  
199  
200  
201  
202  
203  
204  
205  
206  
207  
208  
209  
210  
211  
212  
213  
214  
215  
216  
217  
218  
219  
220  
221  
222  
223  
224  
225  
226  
227  
228  
229  
230  
231  
232  
233  
234  
235  
236  
237  
238  
239  
240  
241  
242  
243  
244  
245  
246  
247  
248  
249  
250  
251  
252  
253  
254  
255  
256  
257  
258  
259  
260  
261  
262  
263  
264  
265  
266  
267  
268  
269  
270  
271  
272  
273  
274  
275  
276  
277  
278  
279  
280  
281  
282  
283  
284  
285  
286  
287  
288  
289  
290  
291  
292  
293  
294  
295  
296  
297  
298  
299  
300  
301  
302  
303  
304  
305  
306  
307  
308  
309  
310  
311  
312  
313  
314  
315  
316  
317  
318  
319  
320  
321  
322  
323  
324  
325  
326  
327  
328  
329  
330  
331  
332  
333  
334  
335  
336  
337  
338  
339  
340  
341  
342  
343  
344  
345  
346  
347  
348  
349  
350  
351  
352  
353  
354  
355  
356  
357  
358  
359  
360  
361  
362  
363  
364  
365  
366  
367  
368  
369  
370  
371  
372  
373  
374  
375  
376  
377  
378  
379  
380  
381  
382  
383  
384  
385  
386  
387  
388  
389  
390  
391  
392  
393  
394  
395  
396  
397  
398  
399  
400  
401  
402  
403  
404  
405  
406  
407  
408  
409  
410  
411  
412  
413  
414  
415  
416  
417  
418  
419  
420  
421  
422  
423  
424  
425  
426  
427  
428  
429  
430  
431  
432  
433  
434  
435  
436  
437  
438  
439  
440  
441  
442  
443  
444  
445  
446  
447  
448  
449  
450  
451  
452  
453  
454  
455  
456  
457  
458  
459  
460  
461  
462  
463  
464  
465  
466  
467  
468  
469  
470  
471  
472  
473  
474  
475  
476  
477  
478  
479  
480  
481  
482  
483  
484  
485  
486  
487  
488  
489  
490  
491  
492  
493  
494  
495  
496  
497  
498  
499  
500  
501  
502  
503  
504  
505  
506  
507  
508  
509  
510  
511  
512  
513  
514  
515  
516  
517  
518  
519  
520  
521  
522  
523  
524  
525  
526  
527  
528  
529  
530  
531  
532  
533  
534  
535  
536  
537  
538  
539  
540  
541  
542  
543  
544  
545  
546  
547  
548  
549  
550  
551  
552  
553  
554  
555  
556  
557  
558  
559  
560  
561  
562  
563  
564  
565  
566  
567  
568  
569  
570  
571  
572  
573  
574  
575  
576  
577  
578  
579  
580  
581  
582  
583  
584  
585  
586  
587  
588  
589  
590  
591  
592  
593  
594  
595  
596  
597  
598  
599  
600  
601  
602  
603  
604  
605  
606  
607  
608  
609  
610  
611  
612  
613  
614  
615  
616  
617  
618  
619  
620  
621  
622  
623  
624  
625  
626  
627  
628  
629  
630  
631  
632  
633  
634  
635  
636  
637  
638  
639  
640  
641  
642  
643  
644  
645  
646  
647  
648  
649  
650  
651  
652  
653  
654  
655  
656  
657  
658  
659  
660  
661  
662  
663  
664  
665  
666  
667  
668  
669  
670  
671  
672  
673  
674  
675  
676  
677  
678  
679  
680  
681  
682  
683  
684  
685  
686  
687  
688  
689  
690  
691  
692  
693  
694  
695  
696  
697  
698  
699  
700  
701  
702  
703  
704  
705  
706  
707  
708  
709  
710  
711  
712  
713  
714  
715  
716  
717  
718  
719  
720  
721  
722  
723  
724  
725  
726  
727  
728  
729  
730  
731  
732  
733  
734  
735  
736  
737  
738  
739  
740  
741  
742  
743  
744  
745  
746  
747  
748  
749  
750  
751  
752  
753  
754  
755  
756  
757  
758  
759  
760  
761  
762  
763  
764  
765  
766  
767  
768  
769  
770  
771  
772  
773  
774  
775  
776  
777  
778  
779  
780  
781  
782  
783  
784  
785  
786  
787  
788  
789  
790  
791  
792  
793  
794  
795  
796  
797  
798  
799  
800  
801  
802  
803  
804  
805  
806  
807  
808  
809  
8010  
8011  
8012  
8013  
8014  
8015  
8016  
8017  
8018  
8019  
8020  
8021  
8022  
8023  
8024  
8025  
8026  
8027  
8028  
8029  
8030  
8031  
8032  
8033  
8034  
8035  
8036  
8037  
8038  
8039  
8040  
8041  
8042  
8043  
8044  
8045  
8046  
8047  
8048  
8049  
8050  
8051  
8052  
8053  
8054  
8055  
8056  
8057  
8058  
8059  
8060  
8061  
8062  
8063  
8064  
8065  
8066  
8067  
8068  
8069  
8070  
8071  
8072  
8073  
8074  
8075  
8076  
8077  
8078  
8079  
8080  
8081  
8082  
8083  
8084  
8085  
8086  
8087  
8088  
8089  
8090  
8091  
8092  
8093  
8094  
8095  
8096  
8097  
8098  
8099  
80100  
80101  
80102  
80103  
80104  
80105  
80106  
80107  
80108  
80109  
80110  
80111  
80112  
80113  
80114  
80115  
80116  
80117  
80118  
80119  
80120  
80121  
80122  
80123  
80124  
80125  
80126  
80127  
80128  
80129  
80130  
80131  
80132  
80133  
80134  
80135  
80136  
80137  
80138  
80139  
80140  
80141  
80142  
80143  
80144  
80145  
80146  
80147  
80148  
80149  
80150  
80151  
80152  
80153  
80154  
80155  
80156  
80157  
80158  
80159  
80160  
80161  
80162  
80163  
80164  
80165  
80166  
80167  
80168  
80169  
80170  
80171  
80172  
80173  
80174  
80175  
80176  
80177  
80178  
80179  
80180  
80181  
80182  
80183  
80184  
80185  
80186  
80187  
80188  
80189  
80190  
80191  
80192  
80193  
80194  
80195  
80196  
80197  
80198  
80199  
80200  
80201  
80202  
80203  
80204  
80205  
80206  
80207  
80208  
80209  
80210  
80211  
80212  
80213  
80214  
80215  
80216  
80217  
80218  
80219  
80220  
80221  
80222  
80223  
80224  
80225  
80226  
80227  
80228  
80229  
80230  
80231  
80232  
80233  
80234  
80235  
80236  
80237  
80238  
80239  
80240  
80241  
80242  
80243  
80244  
80245  
80246  
80247  
80248  
80249  
80250  
80251  
80252  
80253  
80254  
80255  
80256  
80257  
80258  
80259  
80260  
80261  
80262  
80263  
80264  
80265  
80266  
80267  
80268  
80269  
80270  
80271  
80272  
80273  
80274  
80275  
80276  
80277  
80278  
80279  
80280  
80281  
80282  
80283  
80284  
80285  
80286  
80287  
80288  
80289  
80290  
80291  
80292  
80293  
80294  
80295  
80296  
80297  
80298  
80299  
80300  
80301  
80302  
80303  
80304  
80305  
80306  
80307  
80308  
80309  
80310  
80311  
80312  
80313  
80314  
80315  
80316  
80317  
80318  
80319  
80320  
80321  
80322  
80323  
80324  
80325  
80326  
80327  
80328  
80329  
80330  
80331  
80332  
80333  
80334  
80335  
80336  
80337  
80338  
80339  
80340  
80341  
80342  
80343  
80344  
80345  
80346  
80347  
80348  
80349  
80350  
80351  
80352  
80353  
80354  
80355  
80356  
80357  
80358  
80359  
80360  
80361  
80362  
80363  
80364  
80365  
80366  
80367  
80368  
80369  
80370  
80371  
80372  
80373  
80374  
80375  
80376  
80377  
80378  
80379  
80380  
80381  
80382  
80383  
80384  
80385  
80386  
80387  
80388  
80389  
80390  
80391  
80392  
80393  
80394  
80395  
80396  
80397  
80398  
80399  
80400  
80401  
80402  
80403  
80404  
80405  
80406  
80407  
80408  
80409  
80410  
80411  
80412  
80413  
80414  
80415  
80416  
80417  
80418  
80419  
80420  
80421  
80422  
80423  
80424  
80425  
80426  
80427  
80428  
80429  
80430  
80431  
80432  
80433  
80434  
80435  
80436  
80437  
80438  
80439  
80440  
80441  
80442  
80443  
80444  
80445  
80446  
80447  
80448  
80449  
80450  
80451  
80452  
80453  
80454  
80455  
80456  
80457  
80458  
80459  
80460  
80461  
80462  
80463  
80464  
80465  
80466  
80467  
80468  
80469  
80470  
80471  
80472  
80473  
80474  
80475  
80476  
80477  
80478  
80479  
80480  
80481  
80482  
80483  
80484  
80485  
80486  
80487  
80488  
80489  
80490  
80491  
80492  
80493  
80494  
80495  
80496  
80497  
80498  
80499  
80500  
80501  
80502  
80503  
80504  
80505  
80506  
80507  
80508  
80509  
80510  
80511  
80512  
80513  
80514  
80515  
80516  
80517  
80518  
80519  
80520  
80521  
80522  
80523  
80524  
80525  
80526  
80527  
80528  
80529  
80530  
80531  
80532  
80533  
80534  
80535  
80536  
80537  
80538  
80539  
80540  
80541  
80542  
80543  
80544  
80545  
80546  
80547  
80548  
80549  
80550  
80551  
80552  
80553  
80554  
80555  
80556  
80557  
80558  
80559  
80560  
80561  
80562  
80563  
80564  
80565  
80566  
80567  
80568  
80569  
80570  
80571  
80572  
80573  
80574  
80575  
80576  
80577  
80578  
80579  
80580  
80581  
80582  
80583  
80584  
80585  
80586  
80587  
80588  
80589  
80590  
80591  
80592  
80593  
80594  
80595  
80596  
80597  
80598  
80599  
80600  
80601  
80602  
80603  
80604  
80605  
80606  
80607  
80608  
80609  
80610  
80611  
80612  
80613  
80614  
80615  
80616  
80617  
80618  
80619  
80620  
80621  
80622  
80623  
80624  
80625  
80626  
80627  
80628  
80629  
80630  
80631  
80632  
80633  
80634  
80635  
80636  
80637  
80638  
80639  
80640  
80641  
80642  
80643  
80644  
80645  
80646  
80647  
80648  
80649  
80650  
80651  
80652  
80653  
80654  
80655  
80656  
80657  
80658  
80659  
80660  
80661  
80662  
80663  
80664  
80665  
80666  
80667  
80668  
80669  
80670  
80671  
80672  
80673  
80674  
80675  
80676  
80677  
80678  
80679  
80680  
80681  
80682  
80683  
80684  
80685  
80686  
80687  
80688  
80689  
80690  
80691  
80692  
80693  
80694  
80695  
80696  
80697  
80698  
80699  
80700  
80701  
80702  
80703  
80704  
80705  
80706  
80707  
80708  
80709  
80710  
80711  
80712  
80713  
80714  
80715  
80716  
80717  
80718  
80719  
80720  
80721  
80722  
80723  
80724  
80725  
80726  
80727  
80728  
80729  
80730  
80731  
80732  
80733  
80734  
80735  
80736  
80737  
80738  
80739  
80740  
80741  
80742  
80743  
80744  
80745  
80746  
80747  
80748  
80749  
80750  
80751  
80752  
80753  
80754  
80755  
80756  
80757  
80758  
80759  
80760  
80761  
80762  
80763  
80764  
80765  
80766  
80767  
80768  
80769  
80770  
80771  
80772  
80773  
80774  
80775  
80776  
80777  
80778  
80779  
80780  
80781  
80782  
80783  
80784  
80785  
80786  
80787  
80788  
80789  
80790  
80791  
80792  
80793  
80794  
80795  
80796  
80797  
80798  
80799  
80800  
80801  
80802  
80803  
80804  
80805  
80806  
80807  
80808  
80809  
80810  
80811  
80812  
80813  
80814  
80815  
80816  
80817  
80818  
80819  
80820  
80821  
80822  
80823  
80824  
80825  
80826  
80827  
80828  
80829  
80830  
80831  
80832  
80833  
80834  
80835  
80836  
80837  
80838  
80839  
80840  
80841  
80842  
80843  
80844  
80845  
80846  
80847  
80848  
80849  
80850  
80851  
80852  
80853  
80854  
80855  
80856  
80857  
80858  
80859  
80860  
80861  
80862  
80863  
80864  
80865  
80866  
80867  
80868  
80869  
80870  
80871  
80872  
80873  
80874  
80875  
80876  
80877  
80878  
80879  
80880  
80881  
80882  
80883  
80884  
80885  
80886  
80887  
80888  
80889  
80890  
80891  
80892  
80893  
80894  
80895  
80896  
80897  
80898  
80899  
80900  
80901  
80902  
80903  
80904  
80905  
80906  
80907  
80908  
80909  
80910  
80911  
80912  
80913  
80914  
80915  
80916  
80917  
80918  
80919  
80920  
80921  
80922  
80923  
80924  
80925  
80926  
80927  
80928  
80929  
80930  
80931  
80932  
80933  
80934  
80935  
80936  
80937  
80938  
80939  
80940  
80941  
80942  
80943  
80944  
80945  
80946  
80947  
80948  
80949  
80950  
80951  
80952  
80953  
80954  
80955  
80956  
80957  
80958  
80959  
80960  
80961  
80962  
80963  
80964  
80965  
80966  
80967  
80968  
80969  
80970  
80971  
80972  
80973  
80974  
80975  
80976  
80977  
80978  
80979  
80980  
80981  
80982  
80983  
80984  
80985  
80986  
80987  
80988  
80989  
80990  
80991  
80992  
80993  
80994  
80995  
80996  
80997  
80998  
80999  
80100  
80101

glass was then heated and cooled two additional times. All heating and cooling was performed at 5 K/min. As expected based on previous results<sup>42</sup>, the PVD glass is thinner and thus denser than the liquid-cooled glass. Additionally, the PVD glass has a higher refractive index. Since ethylbenzene glasses can be anisotropic (birefringence is discussed below) we report the mean-squared refractive index,<sup>42-43</sup>  $\langle n^2 \rangle$ , as follows:

$$\langle n^2 \rangle = \frac{n_e^2 + 2n_o^2}{3} \quad (1)$$

Here,  $n_e$  is the refractive index out of the plane of the substrate and  $n_o$  is the refractive index in the plane of the substrate. Figure 2 also illustrates the definition of the fictive temperature ( $T_f$ ). We extrapolate the fitted line of the supercooled liquid to intersect the as-deposited glass curve; the intersection point is  $T_f$ . Each experiment yields two fictive temperatures, characterizing the density and refractive index of the vapor-deposited glass;  $T_f = T_{\text{sub}}$  means that the as-deposited glass has the density or refractive index expected for the (extrapolated) supercooled liquid.

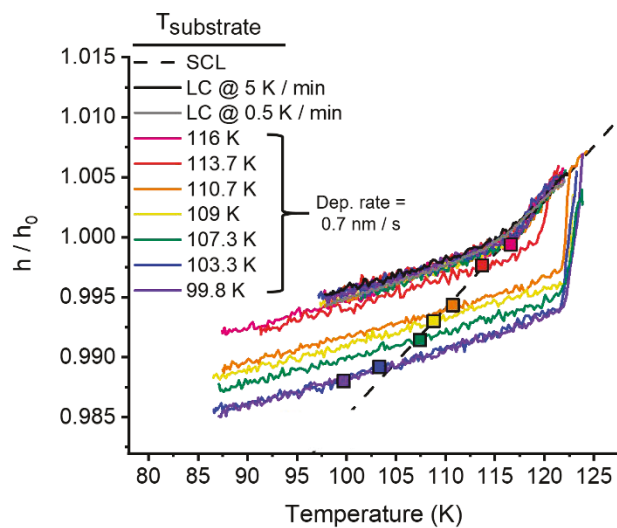


1  
2  
3  
4  
5  
6  
7  
8  
9  
10  
11  
12  
13  
14  
15  
16  
17  
18  
19  
20  
21  
22  
23  
24  
25  
26  
27  
28  
29  
30  
31  
32  
33  
34  
35  
36  
37  
38  
39  
40  
41  
42  
43  
44  
45  
46  
47  
48  
49  
50  
51  
52  
53  
54  
55  
56  
57  
58  
59  
60

*Figure 2. In situ ellipsometry data from ramping experiments of ethylbenzene deposited at  $T_{sub} = 103.3$  K (0.89  $T_g$ ) with a rate of 0.7 nm/s illustrating the increased density and kinetic stability of the PVD glass. The top panel shows the thickness of the as-deposited glass in comparison with the liquid-cooled glass. The bottom panel shows mean-squared refractive index ( $\langle n^2 \rangle$ ). The black dashed lines are fits to the data for the glasses and supercooled liquid. The intersection of the extrapolated supercooled liquid line and as-deposited glass fit defines the fictive temperature,  $T_f$ . The intersection of the supercooled liquid and liquid-cooled glass fits define  $T_g$ . The structure of ethylbenzene is shown in the bottom panel.*

Figure 3 compares all glasses of ethylbenzene deposited at 0.7 nm/s over a range of substrate temperatures and illustrates that PVD glasses prepared with substrate temperatures as low as 107 K have densities consistent with the supercooled liquid. The colored curves show the normalized thickness change of the as-deposited glasses upon initial heating and the subsequent heating scan for the corresponding liquid-cooled glass. The change in thickness is inversely proportional to the change in density. The black and grey curves show data for liquid-cooled glasses prepared at two cooling rates, 5 K/min and 0.5 K/min, respectively. The solid points show the normalized change in thickness at each substrate temperature. The black dashed line is the extrapolation of the equilibrium supercooled liquid. Down to substrate temperatures of 107.3 K, the PVD glasses prepared with a deposition rate of 0.7 nm/s have densities consistent with those

expected for the supercooled liquid. This substrate temperature range also results in PVD glasses with enthalpies that are consistent with high temperature extrapolations.<sup>33</sup> For substrate temperatures below 107.3 K, deposition at 0.7 nm/s does not produce glasses that have densities consistent with those expected for the supercooled liquid (as illustrated by the colored squares that do not lie on the line).



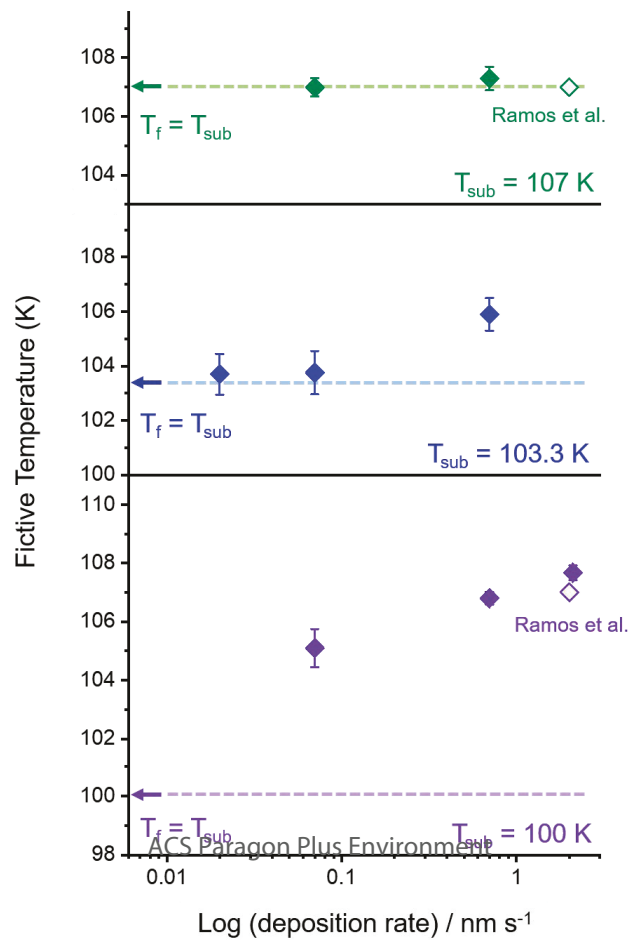
1  
2  
3  
4  
5  
6  
7 *Figure 3. Normalized change in thickness as a function of temperature for glasses of ethylbenzene*  
8 *deposited at 0.7 nm/s. The colored curves represent PVD glasses prepared at the indicated*  
9 *substrate temperatures. The heating curve for the as-deposited glass and the first heating curve*  
10 *for the corresponding liquid-cooled glass are shown. The black and grey curves show results for*  
11 *liquid-cooled glasses cooled at 5 K/min and 0.5 K/min, respectively. The black dashed line is the*  
12 *extrapolation of the equilibrium supercooled liquid. Colored squares represent the normalized*  
13 *change in thickness at the deposition temperature. When these squares lie on the dashed line, the*  
14 *densities measured are consistent with the density expected for the supercooled liquid. For clarity,*  
15 *only the glasses prepared with a deposition rate of 0.7 nm/s are shown.*

16  
17  
18  
19  
20  
21

22 Figure 4 illustrates how lower deposition rates can be used to increase the range of substrate  
23 temperatures for which the extrapolated supercooled liquid density is attained. For glasses  
24 deposited at 107 K (green, top panel), films prepared at two different rates have fictive  
25 temperatures equal to the substrate temperature; we interpret this to mean that both rates are slow  
26 enough to achieve the equilibrium density during deposition. For glasses deposited at 103.3 K  
27 (blue, middle panel), lowering the deposition rate from 0.7 nm/s produces denser glasses as  
28 indicated by the lower fictive temperatures. The good agreement between fictive temperatures for  
29 the two slower depositions suggests that the equilibrium density is attained already with the  
30 intermediate deposition rate. For the lowest substrate temperature shown, 100 K (purple, bottom  
31 panel), lowering the deposition rate smoothly increases the density. We conclude that even lower  
32 deposition rates would be required to reach the equilibrium density. The fictive temperatures in  
33 Figure 4 are in excellent agreement with those obtained from the enthalpy measurements of Ramos  
34 et al.<sup>33</sup> In comparison with reference <sup>33</sup>, lower deposition rates could be achieved with the  
35 ellipsometry measurements since much thinner films can be utilized, allowing us to extend the  
36 temperature range where PVD glass properties match those of the extrapolated supercooled liquid.

37  
38  
39  
40  
41  
42  
43  
44  
45  
46  
47  
48  
49  
50  
51  
52  
53  
54  
55  
56  
57  
58  
59  
60

Based on the extrapolation of Tatsumi et al.<sup>8</sup>, equilibration at 103.3 K instead of 105 K lowers the configurational entropy by 30%.



1  
2  
3  
4  
5  
6  
7  
8  
9  
10  
11  
12  
13  
14  
15  
16  
17  
18  
19  
20  
21  
22  
23  
24  
25  
26  
27  
28  
29  
30  
31  
32  
33  
34  
35  
36  
37  
38  
39  
40  
41  
42  
43  
44  
45  
46  
47  
48  
49  
50  
51  
52  
53  
54  
55  
56  
57  
58  
59  
60

*Figure 4. Fictive temperatures as a function of deposition rate for ethylbenzene glasses deposited at 107 K (green, top), 103.3 K (blue, middle) and 100 K (purple, bottom). The solid points are fictive temperatures calculated from density measurements. Arrows and dashed lines indicate where  $T_f = T_{sub}$ . The open points represent enthalpy measurements by Ramos et al.<sup>33</sup>*

By utilizing lower deposition rates, ethylbenzene glasses can be prepared that have properties consistent with the extrapolated supercooled liquid down to a temperature only a few Kelvin above  $T_K$ . Figure 5 illustrates the fictive temperatures of glasses prepared with a range of substrate temperatures and deposition rates. The black dashed line shows  $T_f = T_{sub}$ ; the points that fall on this line represent glasses that have properties consistent with those expected for the supercooled liquid. Three different properties are compared in Figure 5. The colored points show fictive temperatures for the density and refractive index for the ethylbenzene glasses prepared in this work. The black squares represent the enthalpy measurements of Ramos et al.<sup>33</sup> for glasses deposited at 2 nm/s. There is excellent agreement between the fictive temperatures calculated from these three observables. In other words, in the limit of low deposition rates, the density, enthalpy, and refractive index of vapor-deposited glasses are all consistent with the values expected for the

supercooled liquid. Figure 5 establishes that PVD glasses of ethylbenzene can approach the limit of “ideal glass” packing. The glasses deposited at 0.02 nm/s at  $T_{\text{sub}} = 103.3$  K are only 0.15% less dense than the ideal glass (based upon extrapolation to 101 K).

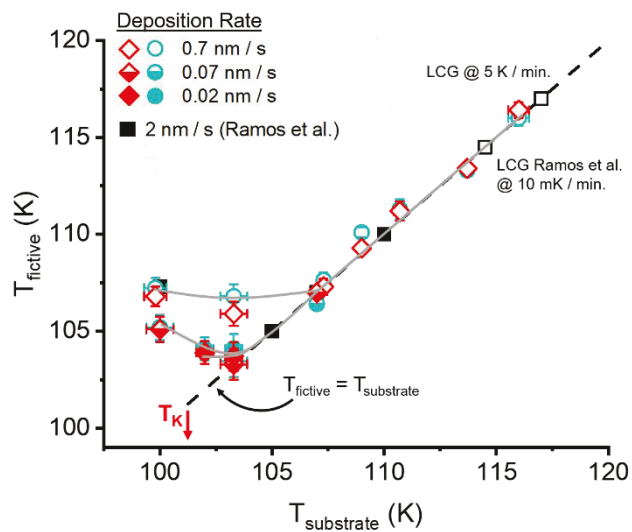


Figure 5. Fictive temperature as a function of substrate temperature during deposition for ethylbenzene glasses prepared at several rates. At low deposition rates, PVD glasses have the properties expected for the supercooled liquid to within 2 K of  $T_K$ . Red symbols are calculated from thickness measurements, teal symbols are calculated from refractive index measurements, and black squares from enthalpy measurements.<sup>33</sup> Open squares represent liquid-cooled glasses with cooling rates indicated. The arrow indicates the location of  $T_K$  as reported by Ref. <sup>8</sup>. The grey solid lines are guides to the eye illustrating trends for different deposition rates.

While Figure 5 illustrates the progress gained toward the Kauzmann temperature by depositing glasses more slowly, it is worth noting that there is potential uncertainty in the value of  $T_K$ . Based upon adiabatic calorimetry data on the crystal, supercooled liquid, and liquid-cooled glass of ethylbenzene, Yamamuro et al. reported a Kauzmann temperature of 101 K.<sup>8</sup> Their calculation of the configurational entropy of the supercooled liquid includes a term that corrects

1  
2  
3 for the difference in vibrational entropy between the glass and crystal. However, recent work<sup>36</sup> has  
4 shown that PVD glasses of ethylbenzene deposited near 103 K have heat capacities in the  
5 temperature range just below  $T_g$  that are roughly 2.5% lower than a liquid-cooled glass. If we  
6 accept that the highest density vapor-deposited glass is a better model for the ideal glass than is  
7 the liquid-cooled glass, the value of  $T_K$  will shift. To estimate the magnitude of this correction,  
8 we apply the 2.5% decrease in heat capacity in the temperature window from 90 K to 116 K.  
9 Previous work has shown a correlation between the diminished heat capacity and suppression of  
10 secondary relaxations in PVD glasses of toluene,<sup>44</sup> and the temperature window above is a  
11 reasonable estimate of the regime where secondary relaxations might contribute to the heat  
12 capacity of the liquid-cooled glass of ethylbenzene.<sup>45</sup> Accounting for this difference in heat  
13 capacity, Yamamuro et al.'s value of  $T_K$  is lowered by 0.7 K, to just above 100 K. Our  
14 recalculation of  $T_K$  clearly makes a significant assumption that could be tested with heat capacity  
15 measurements on PVD glasses over a wide temperature range.  
16  
17

18 One potential criticism of PVD glasses serving as models for the supercooled liquid is that  
19 deposited glasses can be anisotropic.<sup>42, 46-48</sup> Thus, the birefringence of these PVD glasses (also  
20 obtained from ellipsometry) provides a further test of the extent to which the as-deposited films  
21 have the structure expected for the supercooled liquid. Birefringence values for glasses deposited  
22 at all substrate temperatures and deposition rates are shown in Figure 6. For substrate temperatures  
23 above 109 K, all the as-deposited glasses are isotropic within measurement error. At lower  
24 substrate temperatures, the glasses are birefringent, with the maximum value equal to 0.02. In this  
25 regime, as the deposition rate is lowered, the birefringence values decrease significantly. This  
26 behavior supports the view that PVD glasses approach the isotropic structure of the supercooled  
27 liquid in the limit of low deposition rates.  
28  
29  
30  
31  
32  
33  
34  
35  
36  
37  
38  
39  
40  
41  
42  
43  
44  
45  
46  
47  
48  
49  
50  
51  
52  
53  
54  
55  
56  
57  
58  
59  
60

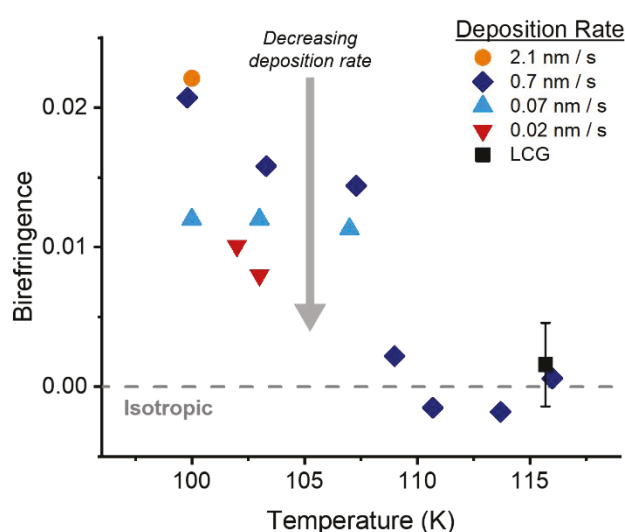


Figure 6. Birefringence as a function of substrate temperature for vapor-deposited glasses of ethylbenzene, with deposition rates indicated in the legend. The black open square is the average birefringence of all glasses prepared by cooling the liquid at 5 K/min; the error bar indicates one standard deviation. Error bars for the PVD glasses are expected to be comparable.

The results presented here are significant in establishing that PVD glasses can be useful models for the equilibrium supercooled liquid. We have shown that the density and refractive index values obtained in the limit of low deposition rates are consistent with those expected for the supercooled liquid down to 103 K. By combining our results with previous measurements, we show that the density, refractive index, and enthalpy of PVD ethylbenzene glasses all have the values expected for the equilibrium supercooled liquid down to 105 K. While the glasses obtained at 103 K are mildly anisotropic, those prepared at the lowest deposition rate are substantially more isotropic than those prepared at higher deposition rates. These results, taken together, strongly suggest that the properties of the supercooled liquid, obtained by extrapolation from above  $T_g$ , are accurate down to a few Kelvin above  $T_g$ .

1  
2  
3 These new results on PVD glasses provide insight into the resolution of the Kauzmann  
4 entropy crisis. At some point, the extrapolation of the supercooled liquid entropy must fail. Prior  
5 to work on PVD glasses, we understood that the entropy crisis for ethylbenzene should somehow  
6 be resolved between  $T_g$  (116 K) and  $T_K$  (~101 K). As one extreme, the extrapolation might fail  
7 gradually as the temperature is lowered below  $T_g$  with continuously larger deviations between the  
8 actual supercooled liquid properties and those obtained by extrapolation. At the opposite extreme,  
9 the extrapolation might fail at the lowest possible temperature ( $T_K$ ) via a phase transition. The  
10 results presented here on PVD glasses of ethylbenzene, in combination with those from ref <sup>33</sup>,  
11 establish with reasonable certainty that the extrapolated properties of the supercooled liquid of  
12 ethylbenzene are accurate down to within a few Kelvin of  $T_K$ . For this system, the entropy crisis  
13 is not resolved by a gradual failure of the high-temperature extrapolation as temperature is lowered.  
14 Rather, the properties of the supercooled liquid must adjust fairly abruptly below 103 K, either  
15 continuously or via a phase transition. Thus, these experiments on PVD glasses substantially  
16 increase the likelihood of a phase transition to the ideal glass of ethylbenzene at the Kauzmann  
17 temperature. It is possible that other liquids may resolve the entropy crisis differently; for example,  
18 systems exhibiting polyamorphism may undergo a liquid-liquid transition instead.  
19  
20  
21  
22  
23  
24  
25  
26  
27  
28  
29  
30  
31  
32  
33  
34  
35  
36  
37  
38  
39  
40  
41  
42  
43  
44  
45  
46  
47  
48  
49  
50  
51  
52  
53  
54  
55  
56  
57  
58  
59  
60

Based on results in the literature, PVD is most likely to access equilibrated states close to  $T_K$  for low molecular weight systems without hydrogen bonding.<sup>49</sup> In order to test the generality of the results presented here for ethylbenzene, it would be useful for future experiments utilizing low deposition rates to study toluene as there is evidence from calorimetry<sup>34, 37</sup> that glasses with fictive temperatures close to  $T_K$  can also be prepared for this system.

1  
2  
3 **Methods:** Ethylbenzene glasses were prepared by PVD in a vacuum chamber described  
4 previously.<sup>50-52</sup> Ethylbenzene was obtained from Sigma Aldrich (anhydrous, 99.8% purity) and  
5 used without further purification. The molecules are introduced into the vacuum chamber (base  
6 pressure  $\sim 10^{-9}$  torr) via a fine leak valve. All films deposited were about 400 nm thick.  
7  
8

9  
10 For *in situ* ellipsometry measurements, ethylbenzene molecules are deposited directly onto  
11 a 1" silicon wafer with a 25 nm oxide layer. The silicon wafer is in thermal contact via indium foil  
12 with a copper finger cooled by nitrogen gas. The copper finger houses a platinum RTD (resistance  
13 temperature detector) and a cartridge heater that are used to control the temperature of the silicon  
14 wafer in conjunction with a Lakeshore 340 temperature controller. Due to imperfect thermal  
15 contact between the copper finger and the silicon wafer, a correction of 3-4 K was applied to obtain  
16 the temperature of the PVD glass on the silicon wafer. We use the  $T_g$  value obtained upon heating  
17 the liquid-cooled glass (cooling and heating both at 5 K/min) as our reference temperature. Based  
18 upon dielectric relaxation measurements, Chen et al.<sup>35</sup> report that the structural relaxation time has  
19 a value of 100 s at 115.7 K and we use this value for  $T_g$  for the glass prepared by cooling at 5  
20 K/min. All the liquid-cooled glasses discussed in this paper were prepared by cooling at 5 K/min  
21 except for one data set shown in Figure 3 (cooled at 0.5 K/min).  
22  
23

24 Ellipsometry measurements were performed using a J. A. Woollam M-2000U ellipsometer  
25 with an incident angle of 70°. The ellipsometric data were analyzed using an anisotropic Cauchy  
26 model to describe the organic layer and fit in the wavelength range of 350 – 1000 nm. The Cauchy  
27 model is shown in Equation (2) and has been used previously for anisotropic organic films<sup>42</sup>.  
28  
29

30  
31  
32  
33  
34  
35  
36  
37  
38  
39  
40  
41  
42  
43  
44  
45  
46  
47  
48  
49  
50  
51  
52  
53  
54  
55  
56  
57  
58  
59  
60

$$n_o(\lambda) = A_o + \frac{B}{\lambda^2}; n_e(\lambda) = A_e + \frac{B}{\lambda^2} \quad (2)$$

1  
2  
3 During the heterogeneous transformation<sup>42</sup> of vapor-deposited glasses (from 123 to 125 K in  
4 Figure 2), this model is not adequate to quantitatively describe the data; this has no impact on  
5 Figures 4 or 5, or our conclusions.  
6  
7

8  
9 Ellipsometry data was obtained during heating at 5 K/min and was fit following the  
10 procedure outlined in 2001 by Dalnoki-Veress et al.<sup>53</sup> using the function described by Equation  
11  
12 (3):  
13  
14  
15

$$h(T) = w \left( \frac{M - G}{2} \right) \ln \left[ \cosh \left( \frac{T - T_g}{w} \right) \right] + (T - T_g) \left( \frac{M + G}{2} \right) + c \quad (3)$$

16  
17  
18  
19  
20  
21  
22  
23  
24  
25  
26 This fit results in the values of  $T_{\text{onset}}$  for the as-deposited glass and the value of  $T_g$  for the liquid-  
27 cooled glass. The fit also provides the “ $h_0$ ” value used to normalize the data in Figure 3. To obtain  
28 the fictive temperatures for both the thickness and refractive index data, the high-temperature  
29 linear portion of the fit to the supercooled liquid data was extended to intersect with the fit for the  
30 as-deposited glass, similar to the procedure in Reference<sup>54</sup>. Sample fits are provided in the  
31 Supporting Information. Vertical error bars in Figures 4 and 5 represent the error in the  
32 determination of the fictive temperature due to the uncertainty in fitting equation (3). Horizontal  
33 error bars in Figure 5 represent the uncertainty in the temperature. Note that our ellipsometry  
34 measurements were not used to determine absolute densities; the density of the as-deposited glass  
35 relative to the liquid-cooled glass allows the determination of  $T_f$ .  
36  
37  
38  
39  
40  
41  
42  
43  
44  
45  
46  
47

## 51 Acknowledgements

52  
53  
54  
55  
56  
57  
58  
59  
60

We would like to thank Marie Fiori for assistance in analyzing ellipsometry results and  
Diane Walters for experimental assistance. We would also like to thank Ludovic Berthier, Ranko

1  
2  
3 Richert, Birte Riechers, and Amanda Young-Gonzales for helpful discussions. This work was  
4  
5 supported by the U.S. National Science Foundation (Grant No. CHE-1564663 and CHE-1854930).  
6  
7  
8  
9

10 **Supporting Information**  
11

12 Sample fits of ellipsometry data to the model of Dalnoki-Veress et al.<sup>53</sup>.  
13  
14  
15

16 **References**  
17

18  
19 (1) Kauzmann, W., The Nature of the Glassy State and the Behavior of Liquids at Low  
20 Temperatures. *Chem. Rev.* **1948**, *43*, 219-256.  
21  
22 (2) Stillinger, F. H.; Debenedetti, P. G.; Truskett, T. M., The Kauzmann Paradox Revisited.  
23 *The Journal of Physical Chemistry B* **2001**, *105*, 11809-11816.  
24  
25 (3) Gibbs, J. H.; DiMarzio, E. A., Nature of the Glass Transition and the Glassy State. *The*  
26 *Journal of Chemical Physics* **1958**, *28*, 373-383.  
27  
28 (4) Adam, G.; Gibbs, J. H., On the Temperature Dependence of Cooperative Relaxation  
29 Properties in Glass-Forming Liquids. *The Journal of Chemical Physics* **1965**, *43*, 139-146.  
30  
31 (5) Lubchenko, V.; Wolynes, P. G., Theory of Structural Glasses and Supercooled Liquids.  
32 *Annu. Rev. Phys. Chem.* **2007**, *58*, 235-266.  
33  
34 (6) Ninarello, A.; Berthier, L.; Coslovich, D., Models and Algorithms for the Next Generation  
35 of Glass Transition Studies. *Physical Review X* **2017**, *7*, 021039.  
36  
37 (7) Berthier, L.; Ozawa, M.; Scalliet, C., Configurational Entropy of Glass-Forming Liquids.  
38 *The Journal of Chemical Physics* **2019**, *150*, 160902.  
39  
40 (8) Tatsumi, S.; Aso, S.; Yamamuro, O., Thermodynamic Study of Simple Molecular Glasses:  
41 Universal Features in Their Heat Capacity and the Size of the Cooperatively Rearranging Regions.  
42 *Phys. Rev. Lett.* **2012**, *109*, 045701.  
43  
44 (9) Tanaka, H.; Kurita, R.; Mataki, H., Liquid-Liquid Transition in the Molecular Liquid  
45 Triphenyl Phosphite. *Phys. Rev. Lett.* **2004**, *92*, 025701.  
46  
47 (10) Kobayashi, M.; Tanaka, H., The Reversibility and First-Order Nature of Liquid–Liquid  
48 Transition in a Molecular Liquid. *Nature Communications* **2016**, *7*, 13438.  
49  
50 (11) Aasland, S.; McMillan, P. F., Density-Driven Liquid–Liquid Phase Separation in the  
51 System  $\text{Al}_2\text{O}_3$ – $\text{Y}_2\text{O}_3$ . *Nature* **1994**, *369*, 633-636.  
52  
53 (12) Poole, P. H.; Sciortino, F.; Essmann, U.; Stanley, H. E., Phase Behaviour of Metastable  
54 Water. *Nature* **1992**, *360*, 324-328.  
55  
56 (13) Debenedetti, P. G., Supercooled and Glassy Water. *J. Phys.: Condens. Matter* **2003**, *15*,  
57 R1669.  
58  
59 (14) Tanaka, H., Bond Orientational Order in Liquids: Towards a Unified Description of Water-  
60 Like Anomalies, Liquid-Liquid Transition, Glass Transition, and Crystallization. *The European*  
Physical Journal E **2012**, *35*, 113.

(15) Amann-Winkel, K.; Gainaru, C.; Handle, P. H.; Seidl, M.; Nelson, H.; Böhmer, R.; Loerting, T., Water's Second Glass Transition. *Proceedings of the National Academy of Sciences of the United States of America* **2013**, *110*, 17720-17725.

(16) Cohen, M. H.; Grest, G. S., Liquid-Glass Transition, a Free-Volume Approach. *Physical Review B* **1979**, *20*, 1077-1098.

(17) Angell, C. A.; Rao, K. J., Configurational Excitations in Condensed Matter, and the ``Bond Lattice'' Model for the Liquid-Glass Transition. *The Journal of Chemical Physics* **1972**, *57*, 470-481.

(18) Matyushov, D. V.; Angell, C. A., Gaussian Excitations Model for Glass-Former Dynamics and Thermodynamics. *The Journal of Chemical Physics* **2007**, *126*, 094501.

(19) Stillinger, F. H., Supercooled Liquids, Glass Transitions, and the Kauzmann Paradox. *The Journal of Chemical Physics* **1988**, *88*, 7818-7825.

(20) Macedo, P. B.; Capps, W.; Litovitz, T. A., Two-State Model for the Free Volume of Vitreous B<sub>2</sub>O<sub>3</sub>. *The Journal of Chemical Physics* **1966**, *44*, 3357-3364.

(21) Saika-Voivod, I.; Poole, P. H.; Sciortino, F., Fragile-to-Strong Transition and Polyamorphism in the Energy Landscape of Liquid Silica. *Nature* **2001**, *412*, 514-517.

(22) Saika-Voivod, I.; Sciortino, F.; Poole, P. H., Free Energy and Configurational Entropy of Liquid Silica: Fragile-to-Strong Crossover and Polyamorphism. *Physical Review E* **2004**, *69*, 041503.

(23) Saksengwijit, A.; Reinisch, J.; Heuer, A., Origin of the Fragile-to-Strong Crossover in Liquid Silica as Expressed by Its Potential-Energy Landscape. *Phys. Rev. Lett.* **2004**, *93*, 235701.

(24) Wolfgardt, M.; Baschnagel, J.; Paul, W.; Binder, K., Entropy of Glassy Polymer Melts: Comparison between Gibbs-Dimarzio Theory and Simulation. *Physical Review E* **1996**, *54*, 1535-1543.

(25) Yamamuro, O.; Tsukushi, I.; Lindqvist, A.; Takahara, S.; Ishikawa, M.; Matsuo, T., Calorimetric Study of Glassy and Liquid Toluene and Ethylbenzene: Thermodynamic Approach to Spatial Heterogeneity in Glass-Forming Molecular Liquids. *The Journal of Physical Chemistry B* **1998**, *102*, 1605-1609.

(26) Ediger, M. D.; Angell, C. A.; Nagel, S. R., Supercooled Liquids and Glasses. *The Journal of Physical Chemistry* **1996**, *100*, 13200-13212.

(27) Zhao, J.; Simon, S. L.; McKenna, G. B., Using 20-Million-Year-Old Amber to Test the Super-Arrhenius Behaviour of Glass-Forming Systems. *Nature Communications* **2013**, *4*, 1783.

(28) Kob, W.; Berthier, L., Probing a Liquid to Glass Transition in Equilibrium. *Phys. Rev. Lett.* **2013**, *110*, 245702.

(29) Berthier, L.; Jack, R. L., Evidence for a Disordered Critical Point in a Glass-Forming Liquid. *Phys. Rev. Lett.* **2015**, *114*, 205701.

(30) Berthier, L.; Charbonneau, P.; Coslovich, D.; Ninarello, A.; Ozawa, M.; Yaida, S., Configurational Entropy Measurements in Extremely Supercooled Liquids That Break the Glass Ceiling. *Proceedings of the National Academy of Sciences of the United States of America* **2017**, *114*, 11356-11361.

(31) Swallen, S. F.; Kearns, K. L.; Mapes, M. K.; Kim, Y. S.; McMahon, R. J.; Ediger, M. D.; Wu, T.; Yu, L.; Satija, S., Organic Glasses with Exceptional Thermodynamic and Kinetic Stability. *Science* **2007**, *315*, 353-356.

(32) Ediger, M. D., Perspective: Highly Stable Vapor-Deposited Glasses. *The Journal of Chemical Physics* **2017**, *147*, 210901.

(33) Ramos, S. L.; Oguni, M.; Ishii, K.; Nakayama, H., Character of Devitrification, Viewed from Enthalpic Paths, of the Vapor-Deposited Ethylbenzene Glasses. *J. Phys. Chem. B* **2011**, *115*, 14327-14332.

(34) Leon-Gutierrez, E.; Sepúlveda, A.; Garcia, G.; Clavaguera-Mora, M. T.; Rodríguez-Viejo, J., Stability of Thin Film Glasses of Toluene and Ethylbenzene Formed by Vapor Deposition: An In Situ Nanocalorimetric Study. *PCCP* **2010**, *12*, 14693-14698.

(35) Chen, Z.; Richert, R., Dynamics of Glass-Forming Liquids. XV. Dynamical Features of Molecular Liquids That Form Ultra-Stable Glasses by Vapor Deposition. *The Journal of Chemical Physics* **2011**, *135*, 124515.

(36) Ahrenberg, M.; Chua, Y. Z.; Whitaker, K. R.; Huth, H.; Ediger, M. D.; Schick, C., In Situ Investigation of Vapor-Deposited Glasses of Toluene and Ethylbenzene Via Alternating Current Chip-Nanocalorimetry. *The Journal of Chemical Physics* **2013**, *138*, 024501.

(37) Leon-Gutierrez, E.; Sepúlveda, A.; Garcia, G.; Clavaguera-Mora, M. T.; Rodríguez-Viejo, J., Correction: Stability of Thin Film Glasses of Toluene and Ethylbenzene Formed by Vapor Deposition: An in Situ Nanocalorimetric Study. *PCCP* **2016**, *18*, 8244-8245.

(38) Bhattacharya, D.; Sadtchenko, V., Vapor-Deposited Non-Crystalline Phase Vs Ordinary Glasses and Supercooled Liquids: Subtle Thermodynamic and Kinetic Differences. *The Journal of Chemical Physics* **2015**, *142*, 164510.

(39) Ishii, K.; Okamura, T.; Ishikawa, N.; Nakayama, H., A Novel Change of Light Transmission in Supercooled Liquid State of Ethylbenzene. *Chem. Lett.* **2001**, *30*, 52-53.

(40) Ishii, K.; Nakayama, H.; Hirabayashi, S.; Moriyama, R., Anomalously High-Density Glass of Ethylbenzene Prepared by Vapor Deposition at Temperatures Close to the Glass-Transition Temperature. *Chem. Phys. Lett.* **2008**, *459*, 109-112.

(41) Antony, L. W.; Jackson, N. E.; Lyubimov, I.; Vishwanath, V.; Ediger, M. D.; de Pablo, J. J., Influence of Vapor Deposition on Structural and Charge Transport Properties of Ethylbenzene Films. *ACS Central Science* **2017**, *3*, 415-424.

(42) Dalal, S. S.; Ediger, M. D., Molecular Orientation in Stable Glasses of Indomethacin. *The Journal of Physical Chemistry Letters* **2012**, *3*, 1229-1233.

(43) Vuks, M. F., On the Theory of Double Refraction of Liquids and Solution in an Electric Field. *Opt. Spectrosc.* **1966**, *21*, 383-388.

(44) Yu, H. B.; Tylinski, M.; Guiseppi-Elie, A.; Ediger, M. D.; Richert, R., Suppression of Beta Relaxation in Vapor-Deposited Ultrastable Glasses. *Phys. Rev. Lett.* **2015**, *115*, 185501.

(45) Goldstein, M., Viscous Liquids and the Glass Transition. V. Sources of the Excess Specific Heat of the Liquid. *The Journal of Chemical Physics* **1976**, *64*, 4767-4774.

(46) Liu, T.; Exarhos, A. L.; Alguire, E. C.; Gao, F.; Salami-Ranjbaran, E.; Cheng, K.; Jia, T.; Subotnik, J. E.; Walsh, P. J.; Kikkawa, J. M., *et al.*, Birefringent Stable Glass with Predominantly Isotropic Molecular Orientation. *Phys. Rev. Lett.* **2017**, *119*, 095502.

(47) Dalal, S. S.; Walters, D. M.; Lyubimov, I.; de Pablo, J. J.; Ediger, M. D., Tunable Molecular Orientation and Elevated Thermal Stability of Vapor-Deposited Organic Semiconductors. *Proceedings of the National Academy of Sciences of the United States of America* **2015**, *112*, 4227-4232.

(48) Walters, D. M.; Antony, L.; de Pablo, J. J.; Ediger, M. D., Influence of Molecular Shape on the Thermal Stability and Molecular Orientation of Vapor-Deposited Organic Semiconductors. *The Journal of Physical Chemistry Letters* **2017**, *8*, 3380-3386.

1  
2  
3 (49) Tylinski, M.; Chua, Y. Z.; Beasley, M. S.; Schick, C.; Ediger, M. D., Vapor-Deposited  
4 Alcohol Glasses Reveal a Wide Range of Kinetic Stability. *The Journal of Chemical Physics* **2016**,  
5 *145*, 174506.  
6 (50) Whitaker, K. R.; Scifo, D. J.; Ediger, M. D.; Ahrenberg, M.; Schick, C., Highly Stable  
7 Glasses of Cis-Decalin and Cis/Trans-Decalin Mixtures. *The Journal of Physical Chemistry B*  
8 **2013**, *117*, 12724-12733.  
9 (51) Tylinski, M.; Sepulveda, A.; Walters, D. M.; Chua, Y. Z.; Schick, C.; Ediger, M. D., Vapor-  
10 Deposited Glasses of Methyl-M-Toluate: How Uniform Is Stable Glass Transformation? *J. Chem.*  
11 *Phys.* **2015**, *143*, 244509.  
12 (52) Ahrenberg, M.; Shoifet, E.; Whitaker, K. R.; Huth, H.; Ediger, M. D.; Schick, C.,  
13 Differential Alternating Current Chip Calorimeter for in Situ Investigation of Vapor-Deposited  
14 Thin Films. *Rev. Sci. Instrum.* **2012**, *83*, 033902.  
15 (53) Dalnoki-Veress, K.; Forrest, J. A.; Murray, C.; Gigault, C.; Dutcher, J. R., Molecular  
16 Weight Dependence of Reductions in the Glass Transition Temperature of Thin, Freely Standing  
17 Polymer Films. *Physical Review E* **2001**, *63*, 031801.  
18 (54) Zhang, Y.; Woods, C. N.; Alvarez, M.; Jin, Y.; Riggleman, R. A.; Fakhraai, Z., Effect of  
19 Substrate Interactions on the Glass Transition and Length-Scale of Correlated Dynamics in Ultra-  
20 Thin Molecular Glass Films. *The Journal of Chemical Physics* **2018**, *149*, 184902.  
21  
22  
23  
24  
25  
26  
27  
28  
29  
30  
31  
32  
33  
34  
35  
36  
37  
38  
39  
40  
41  
42  
43  
44  
45  
46  
47  
48  
49  
50  
51  
52  
53  
54  
55  
56  
57  
58  
59  
60

**Supporting information:** Vapor-Deposited Ethylbenzene Glasses Approach “Ideal Glass” Density

M.S. Beasley<sup>\*1</sup>, C. Bishop<sup>1</sup>, B.J. Kasting<sup>1</sup>, and M.D. Ediger<sup>1</sup>

<sup>1</sup>Department of Chemistry, University of Wisconsin-Madison, Madison, Wisconsin, 53706, United States

\*Corresponding author

**Fits of ellipsometry data**

In Figure S1 we provide an example showing the fitting procedure used with ellipsometry data obtained during temperature-ramping. The figure shows thickness and refractive index data obtained as the temperature is increased for the same data set shown in Figure 2 of the main text. We fit the data to an equation (S1) described by Dalnoki-Veress et al.<sup>53</sup>

$$h(T) = w \left( \frac{M - G}{2} \right) \ln \left[ \cosh \left( \frac{T - T_g}{w} \right) \right] + (T - T_g) \left( \frac{M + G}{2} \right) + c \quad (S1)$$

This procedure is intended to eliminate potential bias associated with manually extracting  $T_g$  and  $T_{onset}$  values.

Figure S1 illustrates that Equation S1 fits the data well except for the transformation of the as-deposited glass into the supercooled liquid, between 123 K and 125 K. (The non-monotonic behavior displayed in the data over this 2 K range is indicative of transformation via a growth front. The rest of the fit is not affected.) The arrows in Figure S1 indicate the meaning of the values extracted from the fit for  $T_g$ ,  $T_{onset}$ , and  $h_0$ .  $T_g$  is the glass transition temperature for the liquid-cooled glass, obtained upon heating;  $T_{onset}$  is the beginning of the transformation for the PVD glass;  $h_0$  is the thickness at  $T_g$  and is used to normalize the y-axis data in Figure 3. The temperature axis in Figure S1 has been corrected by subtracting the difference between the fitted value of  $T_g$  and the reference  $T_g$  value of 115.7 K. (See methods for details.)

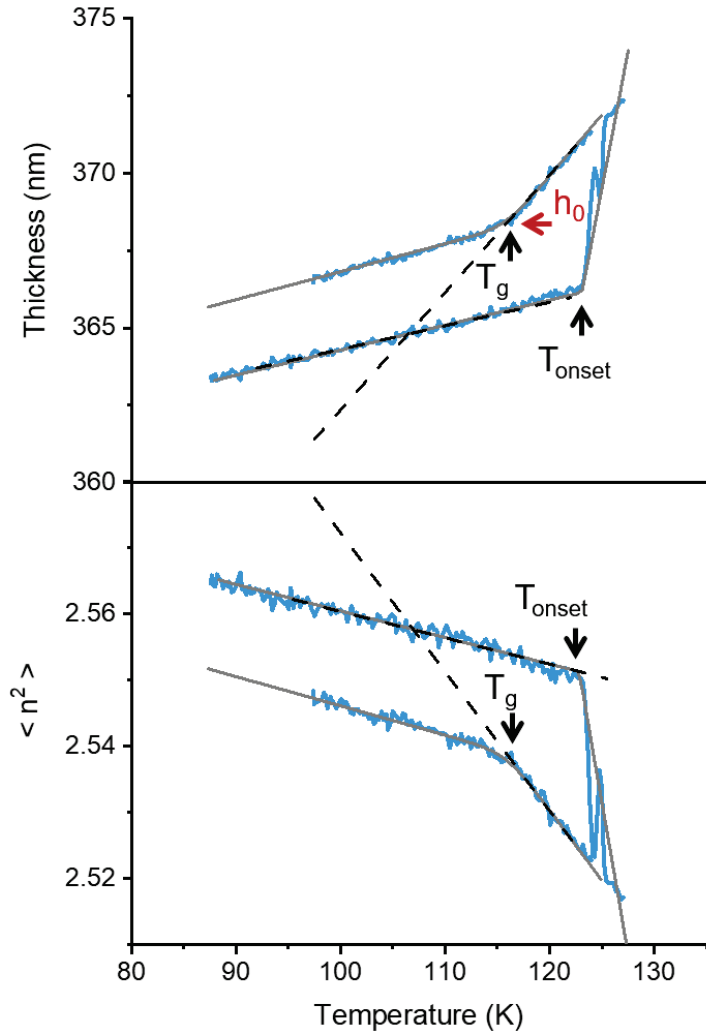


*Figure S1.* Fits of equation S1 to the heating curves for the as-deposited glass and the liquid-cooled glass for the data presented in Figure 2 of the main text. The blue lines are the thickness and refractive index data, the grey lines are the fits to equation S1, and the black dashed lines are linear extrapolations of the fits to the supercooled liquid data. The intersection between the supercooled liquid extrapolation and the glass data defines the fictive temperature  $T_f$ . Arrows indicate values that are extracted from the fits to equation S1.